FULL PAPER

Tunable Color Reflector

ADVANCED
OPTICAL
MATERIALS

www.advopticalmat.de

A Reconfigurable Color Reflector by Selective Phase Change of GeTe in a Multilayer Structure

Mohsen Jafari,* L. Jay Guo,* and Mina Rais-Zadeh

It is shown that a phase change material (PCM), germanium telluride (GeTe), when integrated into a subwavelength layered optical cavity, can produce widely tunable reflective colors. It is shown that the crystallization temperature (T_x) of GeTe is dependent on the film thickness for thin films of less than ≈20 nm, which is exploited for color tuning. Four colors from the same physical structure are demonstrated by electrical heating, through novel optical and thermal engineering of a thin film stack that includes two GeTe layers with only a single integrated joule heater element. The selective sensitivity to incident light angle and low polarization dependence, as well as the low static power consumption of this device make it a good candidate for potential consumer electronics applications.

1. Introduction

Tunable color filters with improved power, speed, and reliability have application in display systems, which are among the most commonly used optical components in consumer market. State-of-the-art active display systems are made based on emitting at a certain wavelength range.[1–4] These active displays, which need constant power to emit at a certain color, are well improved by their technology advancement within the past decades.[5] Among those, light emitting diodes (LEDs) can produce an array of vivid colors and have both improved in quality and cost, leading to their widespread use in commercial products, replacing old liquid crystal display (LCD) technologies.[6,7] However, these seemingly low-power active display systems are still the main source of power usage in electronic devices. Passive displays that only consume power when switching colors are lower power alternatives to active devices, especially in applications requiring low refresh rates.

Most modern display systems use three or more separate subpixels (or cells) to produce a single pixel of an image. Technologies used for producing multicolor pixels include

microelectromechanical (MEMS)-based mirrors,[8] color E-ink,[9] organic light emitting diodes (OLED),[10] etc. However, having a single-cell tunable-color pixel design, which can generate all primary colors, is always desirable for high pixel density displays.[11] An example of this is a single mirror interferometric (SMI) display, where a moving MEMS mirror is used to tune the pixel color in the visible spectrum.[12,13] Having movable objects, however, has proven to be a major limitation of these devices in terms of durability, switching power consumption, and reliability in response to mechanical shocks in portable electronics. To address this, structural color-based filters may be used but cannot provide the whole range of tunable colors.[14] On the other hand, chemical-based color pixels, where an electro-chromatic, a photo-chromatic, or a thermo-chromatic material[15–17] such as a chalcogenide glass[18] is used in a photonic cavity, can provide a more versatile reflective display. Their tunability adds another dimension to the passive or active optical components to achieve smart, light, and durable devices. The gradual change of their optical or electrical properties in the presence of an external stimuli has been demonstrated to be very useful in neuromorphic systems.[19] Recently, an organic-based protein called reflectine, which is extracted from cephalopods, has been used to demonstrate color tuning in the visible, and camouflage in the visible to near-IR ranges in mild environments when durability is not a critical factor.[20]
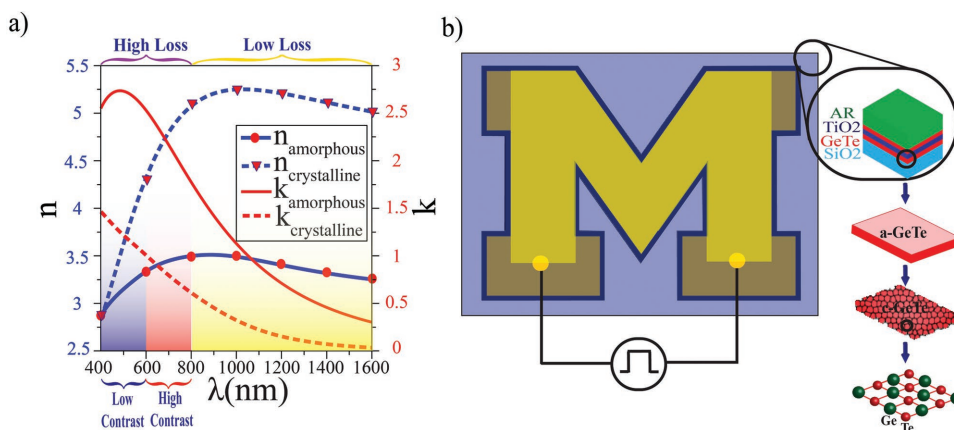
Nonorganic materials such as liquid crystals,[21,22] germanium (antimony) telluride (GeSbTe),[23,24] and vanadium oxide (VO_x)[25] are among the most used materials in reconfigurable optical devices due to the large change in their index of refraction value when switching phases and due to their controllable phase transition processes. GST systems possess two significantly different refractive index values at two different phases due to the existence of resonant bonding in their crystalline structures.[26] Recently, Hosseini et al. introduced a novel type of reflective color filters using a PCM film sandwiched between two indium tin oxide (ITO) electrodes with a bottom reflector.[27] A noteworthy device is demonstrated by Yoo, where a stack consisting of two layers of germanium antimony telluride (GST) is heated using an atomic force microscopy (AFM) tip to achieve more than two colors, although very similar, in single devices.[28,29] Having a lossy layer on top of a metallic reflector with strong interference effect has demonstrated an enhanced sensitivity to refractive index modulation.[30] In this work, we used GeTe in a layered

M. Jafari, Prof. L. J. Guo, Prof. M. Rais-Zadeh
Department of Electrical Engineering and Computer Science
University of Michigan
Ann Arbor, MI 48105, USA
E-mail: jafarim@umich.edu; guo@umich.edu
Prof. M. Rais-Zadeh
NASA Jet Propulsion Laboratory
California Institute of Technology
Pasadena, CA 91109, USA

ADVANCED
SCIENCE NEWS
www.advancedsciencenews.com

ADVANCED
OPTICAL
MATERIALS
www.advopticalmat.de

Figure 1. a) Measured refractive index of GeTe as a function of wavelength in both phases for vis–NIR region. b) Schematic of the device consisting of a buried NiCr heater connected to a gold electrode to apply current. SiO$_2$ phase shift layer (light blue) enhances the color tunability that is achieved as a result of GeTe (red) phase transition. The top AR coating further enhances the color contrast. The color change shown within the "M" sign is due to passing current through integrated heater.
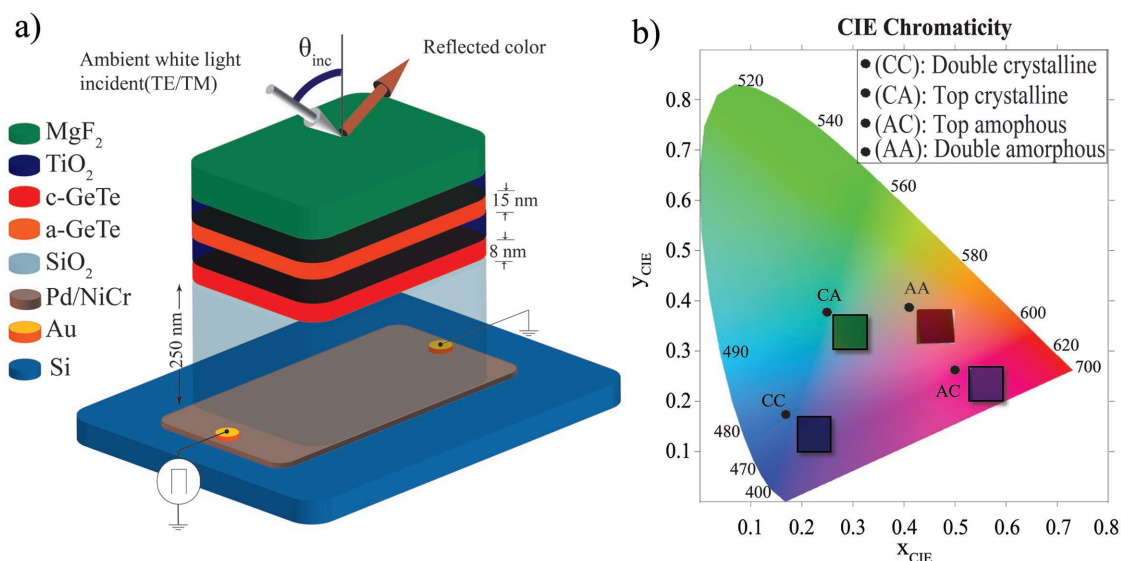
photonic structure to produce a color reflector with four different colors, and achieved electrical switching using an integrated heater. We demonstrate, for the first time, that the phase transition temperature of GeTe is a function of its thickness, and this property was used to selectively change the phase of each thin GeTe within the stack using a single heater line. Different states of color change were achieved using a reversible and localized phase transitioning mechanism with electrical pulses. GeTe offers high temperature stability due to its high phase transition temperature compared to VO$_x$ and GeSbTe. However, the optical loss of GeTe at wavelength range of 400 to 600 nm (marked with blue in **Figure 1**a) must always be considered as a potential limitation for its use in transmission-based devices. Furthermore, as shown in this figure, modulation of the real part of refractive index is negligible, especially around 400 nm. These complications were avoided by making the GeTe layer very thin and utilizing a reflection-based device for ultralow power displays. As a result, four vivid colors were achieved within a single pixel, which have been switched more than 100 times (number of switching cycles restricted by the setup used) with the application of an electrical pulse. GeTe films with thicknesses less than 20 nm were used here to reduce the loss in the visible wavelength. Multilayer devices combining different materials such as VO$_x$ and GST were also studied to achieve narrow-band multireflection states in ref. [31]. It can be perceived that using different thermos-chromic PCMs multicolor could be demonstrated within the single stack. An additional consideration is that unlike VO$_x$ or liquid crystals, both phases of GeTe are stable at room temperature, resulting in zero static power consumption.[32] GeTe, even though a thermo-chromic PCM, could be transitioned electrically[33] or optically,[34] which may prove useful for a diverse field of applications with fully optical operation. One of the main challenges with any reconfigurable device employing a PCM has been to achieve more than two different states even in a multilayer stack. Selective heating of a layer within a thin film stack proves to be impossible even with a dedicated heater for each layer within the stack. In this work, we show four different colors for a thin film stack with two GeTe layers. As mentioned earlier, this unique and selective GeTe phase transitioning method is

obtained using GeTe films with different thickness values sandwiched between titanium dioxide (TiO$_2$) films. Thinner GeTe films with thickness less than 20 nm demonstrate a slightly higher Tx, which helps to realize the multicolor demonstrated in this work using a single heater for the entire stack. Reliable, fast, and repeatable phase transitions are demonstrated for multiple devices showing minimum variation in their optical responses.

2. Results and Discussion

The multilayer device schematic is shown in Figure 1b. The device consists of a two thin GeTe films sitting on top of a SiO$_2$ layer acting as an optical phase shifter. The separation of GeTe from bottom metal with this phase shift layer helps to increase the color contrast. Moreover, it gives the design more flexibility in the positioning of the total light absorption peak within the visible spectrum compared to the devices with GeTe layer directly sitting on a metal substrate.[33,34] Detailed discussion of the device structure design is provided in Section 3 "Methods and Design." Apart from its color tunability, the proposed structure does not require any subwavelength lithography such as those needed in metasurface-based color filters, which results in lower cost needed for large area applications.[30,35] There is a thick palladium/nickel chromium (Pd/NiCr) reflector under the SiO$_2$ layer, which serves as one of the cavity mirror surfaces. Using a refractory metal (palladium) results in higher reliability of the device during repeated heating cycles. This could address the interface degradation and metal diffusion during GeTe phase transition. The GeTe layers on top separated by TiO$_2$ serve as the other semi-Bragg reflector of the cavity. Phase transition of GeTe is controlled using the buried NiCr conductor through joule heating. Engineering the thickness of each layer results in enhanced reflected light sensitivity to the GeTe refractive index which in turn results in a high color contrast that was achieved through only two thin layers of GeTe.

Without losing generality, a two-layer phase change color reflector is discussed here but the number of PCM layers can be increased to increase the number of colors each pixel can

ADVANCED
SCIENCE NEWS

www.advancedsciencenews.com

ADVANCED
OPTICAL
MATERIALS

www.advopticalmat.de

Figure 2. a) Four-color device schematic with the bottom GeTe layer in the crystalline state and the top GeTe layer in the amorphous state (state No. 3 (AC)); b) CIE chromaticity graph showing the device colors in its four different states (CC, CA, AC, and AA).

offer. The device structure is shown in **Figure 2**a and consists of two GeTe layers with 8 and 15 nm thicknesses separated by a 60 nm TiO$_2$ film. The top Magnesium Fluoride (MgF$_2$)(60 nm) and TiO$_2$ (85 nm) films together function as antireflection layer to the 15 nm GeTe film underneath, which increases the color contrast. The cavity was closed on the bottom side by the 100 nm thick reflective palladium and a thin NiCr film used as an adhesive layer.

Furthermore, unlike previous works[27–29] that use direct heating method where GeTe film itself is used to pass the joule heating current, we used a separate heater, which is not in contact with GeTe. In this indirect heating scheme,[36] the current passes through another resistive film (Pd/NiCr) and produces the heat required for crystallographic phase transition. The underlying Pd/NiCr was connected to gold contacts and was used both as the bottom reflector and for joule heating (Figure 1). The indirect heating scheme with no metal in direct contact with GeTe helps to improve the device reliability (achieves more transitions cycles).[37,38] Using this indirect heating approach, selective phase transition was achieved for the two layers of GeTe integrated in the cavity and consequently produced multi reflective colors. The relationship between Tx of GeTe to film thickness was an important consideration for the successful demonstration of indirect heating using a single heater in a device using multiple layers of GeTe. Here, this important feature was used to selectively switch a specific GeTe layer between amorphous and crystalline states, while maintaining all other GeTe layers in their original state. The Tx of GeTe shows an increase as GeTe thickness is decreased for films thinner than ≈20 nm. As a proof of concept, a device consisting of 60 nm of MgF$_2$ antireflection (AR) coating, GeTe layers with 8, 15, and 20 nm thicknesses, 250 nm of SiO$_2$ spacer, and a 100 nm Pd/NiCr reflector is investigated (**Figure 3**a). Each sample was heated to the target temperature shown in the Figure 3b, with a 10 min heating ramp time and was annealed for 30 min at the target temperature. The

samples were then cooled down in a slow 20 min ramp time to room temperature. Figure 3b (photo taken at a 10° angle) compares the reflected colors of these devices at room temperature after annealing. This shows the reflected colors of devices with 8 nm (top row), 15 nm (middle row), and 20 nm (bottom row) thick GeTe films achieving tunable green, red, and blue colors, respectively. As shown in this figure, even though different shades of colors were seen during the partial crystallization of the film, full crystallization happens at different temperature for GeTe films with different thickness. Figure 3c shows these measured Tx for a single layer color reflector with different GeTe film thicknesses. The thicknesses of the films were monitored using ellipsometry with a control sample after each sputtering. The surface morphology of the films was also studied using AFM to ensure that the GeTe layer sputtered over the plasma depositing silicon dioxide layer was uniform as shown in Figure 3c. The surface roughness is measured to be less than 1.5 nm for all sputtered films. This roughness value is small enough to achieve a continuous film as thin as 8 nm needed in this design. To reduce the roughness further, thermal oxide and slower growth of GeTe could also be considered. Figure 3d shows the in situ X-ray diffraction (XRD) of this stack during the phase transitioning of the GeTe films with thicknesses of 8, 15, and 20 nm. To show the crystallization temperature tuning for different thicknesses of GeTe, several samples were analyzed when annealed to a temperature range of 170 to 190 °C inside a high temperature stage filled with N$_2$ gas. An Ultima IV diffractometer (Rigaku Co.) is used to study the in situ XRD of the crystal structures. Fully crystalline GeTe shows a distinctive peak in the XRD intensity pattern at 2θ angle of 30°. As shown here the peak located at 2θ = 30° appears at a higher temperature for a thinner GeTe film compared to those measured for a 20 nm thick GeTe (shown with the horizontal dashed lines). To achieve a better annealing process, several samples were annealed at different temperatures (165 to 190 °C) in a convection oven with nitrogen flow.
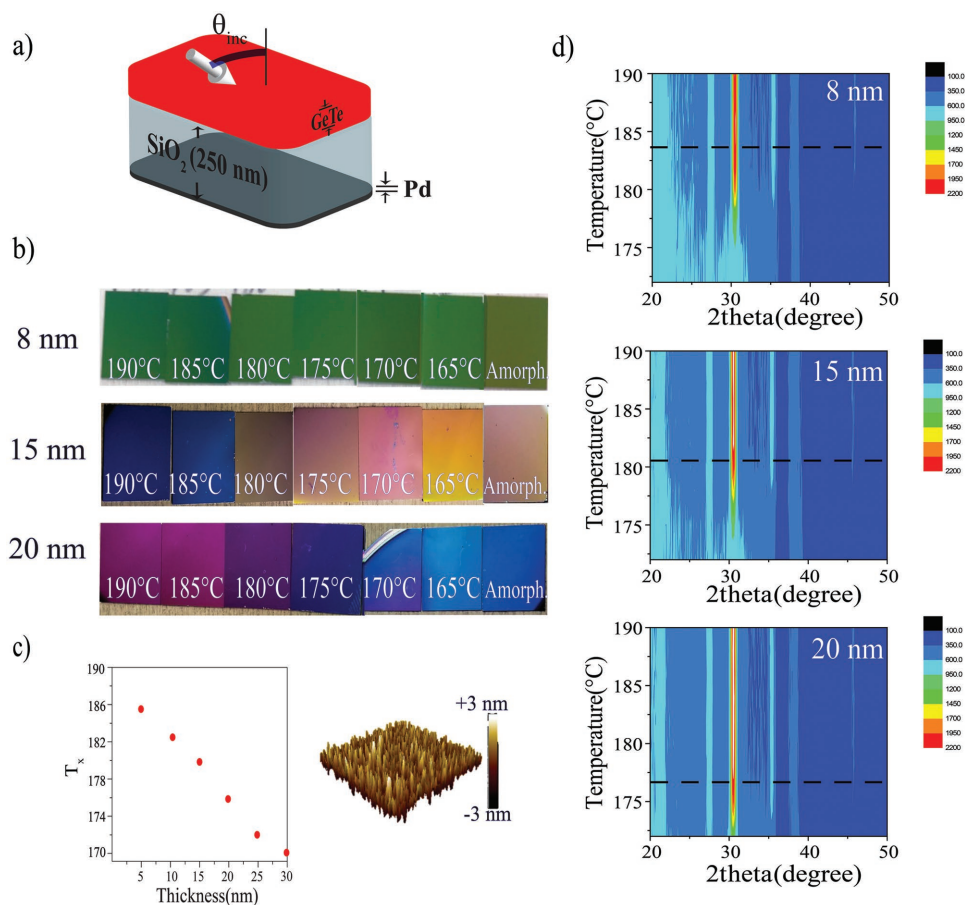
Figure 3. a) The device structure consisting of GeTe, SiO$_2$, and bottom Pd reflector. b) The device color as both a function of temperature and GeTe thickness value (colors are shown for GeTe of 8 nm (top), 15 nm (middle), and 20 nm (bottom) thicknesses). c) Tx variation in devices with different GeTe film thicknesses. Inset: surface morphology using AFM showing <1.5 nm roughness with uniform growth over the surface. d) The color-coded in situ XRD patterns at a temperature range between 170 and 190 °C for devices consisting of GeTe with 8 nm (top row), 15 nm (middle row), and 20 nm (bottom row) thicknesses. The horizontal dashed lines show the complete crystallization for each thickness looking at the XRD peak located at $2\theta = 30°$.
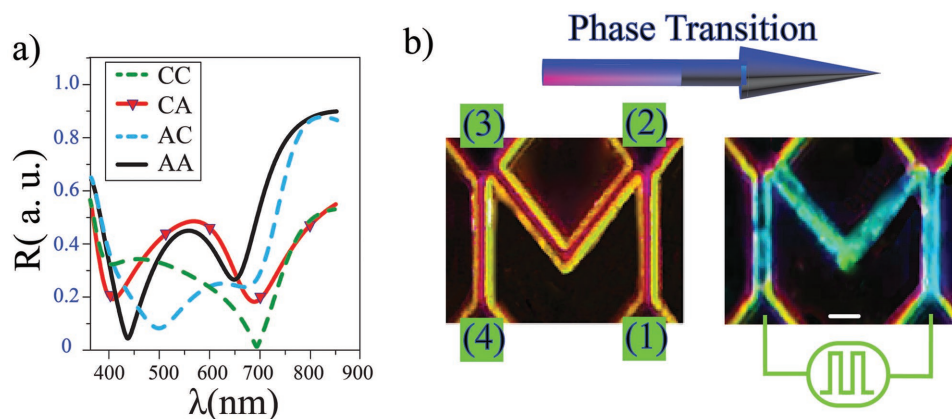
The change in Tx for different film thickness values is most likely due to the fact that the layers in different positions in the z direction of the stack experience different amount of stress applied from the rest of the stack as well as different residual stress within the GeTe layer itself due to the different thickness values. PCMs under stress exhibit different phase transition temperatures than those under no stress, as reported previously in ref. [39]. For the same reason, a highly stressed GeTe film with a thickness larger than 25 nm has a lower phase transition temperature as shown in Figure 3c.

The current for reaching the phase transition temperature is different depending on the metal used for the pads and heater. For Pd heaters with gold pads with a resistance of 80 Ω, full crystallization of both layers is achieved at 186 °C by applying pulses of ≈1 V magnitude, and no damage to the heater or the film stack were observed with more than 2000 pulses applied (see Supporting Information).

Our design provided more than two colors for the whole structure out of two GeTe phases. For example, devices with two GeTe layers demonstrate four stable room temperature states: Both GeTe layers are amorphous (AA); the top layer

amorphous and bottom layer crystalline (AC); top layer crystalline and bottom layer amorphous (CA); both layers are crystalline (CC). One can achieve multiple room temperature stable states by increasing the number of GeTe films. The power consumption for full crystallization (CC) is 12.5 mW for each arm of the "M" sign with an area of 200×10 µm^2. The crystallization pulse for CC state is 1 µs long with a 50% duty cycle (with total period of 2 µs). Therefore, total energy consumption for each crystallization event is 12.5 nJ. The stack discussed here is more susceptible to degradation during the amorphization process (AA) because of the higher temperature needed. The 500 ns voltage pulses of 20 V are used for resetting the devices to original color (AA). Devices consisting of films with lower contamination showed several reset cycles. The required sputtering parameters are mentioned in the Supporting Information. The total energy consumption for each reset process for the area mentioned above is 200 nJ which is due to the lower resistance of the heater after crystallization of the GeTe layers. The CA state was achieved with application of 0.9 V pulses applied for 1 µs with a period of 2 µs heating the device to ≈175 °C. This would keep the top thicker GeTe layer in the

**ADVANCED
SCIENCE NEWS**
www.advancedsciencenews.com

**ADVANCED
OPTICAL
MATERIALS**
www.advopticalmat.de

Figure 4. a) Reflection spectra of the color filter in its four different states for unpolarized light with 50° angle of incidence. The reflection spectrum was measured at room temperature and in ambient light. b) "M" sign color transitioning shown for the right arm when the right pads are used for actuation. 1.5 V voltage pulses are applied for phase transition. Scale bar represents 10 μm.

crystalline state and bottom thin layer in amorphous state. On the other hand, the AC state is achieved by applying a faster pulse with 500 ns width (period: 1 μs) and 1 V amplitude, while keeping the top layer in the amorphous state. More data explaining the rise and fall times of the pulses along with their effect on the heat flow between two GeTe layers were included in Supporting Information.

The measured device reflective color using the chromaticity standard released by International Commission on Illumination (usually abbreviated CIE for its French name, Commission internationale de l'éclairage) at 1931 (CIE-1931) is shown in Figure 2(right). Four distinct colors (dark blue, green, orange, and red as noted by numbers from 1 to 4) were produced by switching the phases of each GeTe films. These colors correspond to double-crystalline, top crystalline, top amorphous, and double amorphous phases of two GeTe thin films.

Device fabrication is discussed in the Supporting Informationin detail. Two of the main challenges with designing a structure with GeTe phase change layer are the design of the heater and selection of a material with proper resistivity and thermal stability. NiCr, which is a thermally stable material with resistivity of 150×10^{-8} Ωm, was used as the heater adjacent to bottom palladium reflector and improved the device reliability and number of successful transition cycles. Noble metals were not used due to low stability at high temperature.

The reflection spectrum of the device was measured using a Woollam M-2000 spectroscopic ellipsometer (JA Woollam Co.). Device reflection responses with a TM polarized light incidence at 50° in both phases of each of two GeTe layers are shown in **Figure 4**a. The experimental data confirms the model used for simulation. This multimode device shows a peak and a dip in the reflection spectrum as shown in Figure 4a. High sensitivity of the dip to the refractive index of GeTe ultrathin film helps to achieve four different spectra in the visible range and thus four different colors.

Figure 4b shows the "M" sign with original red–pink color, which is changed to blue color after transitioning the phase of GeTe layers by applying a current pulse to through the whole "M" heater. Each arm resistance is ≈80 Ω with a total resistance of 200 Ω for the total "M" sign.
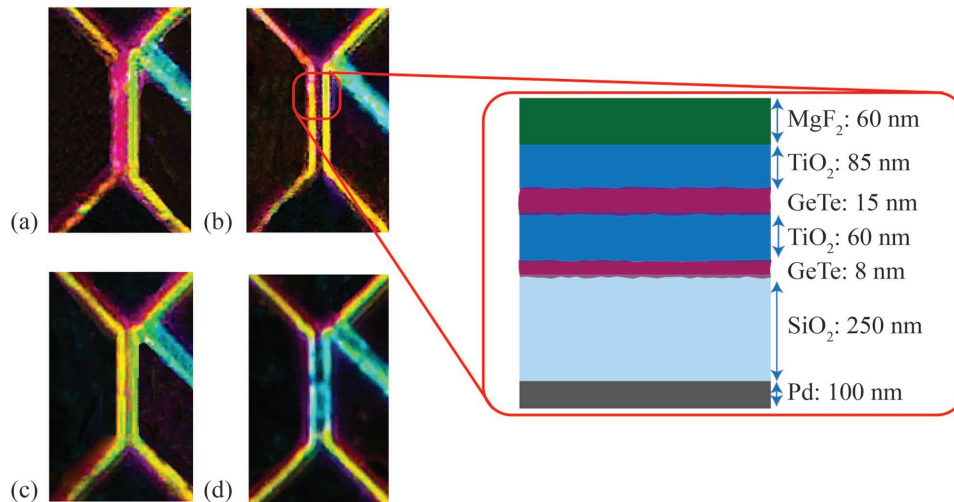
Utilizing such an approach, we demonstrated four different colors for the left arm of the "M" sign as shown in **Figure 5**. Having four different pads to apply electrical pulse we also showed partial phase transitioning for the left arm. Figure 5a shows the color change when Ports (1) and (3) are excited and thus only the three arms in between those ports experience a color change (transitioned to CC). This device is then used to show four different colors in the left arm of the "M" sign. Figure 5a–d shows four different colors: red–pink, yellow, and green–blue, and blue for the left arm of the "M" sign when the bottom pads were excited and current was flowing through the "M" sign. The energy consumption per transition is different for each part of the "M" sign due to resistance change of the arms after phase transition. One can abruptly change the total color of the "M" sign by applying the voltage pulse to the bottom excitation pads (pads labeled (1) and (4) in Figure 4b). Smaller voltage pulses are needed for such an abrupt color change as the resistance of the whole heater is changing abruptly with a single pulse. The sequential process, on the other hand, needs sequential excitation of the pads starting with right and middle arms (Figure 5a), using bottom right (1) and top left (3) pads in Figure 4b), and finally bottom pads (1) and (4).

The reflection spectra versus the incident angles is measured using ellipsometry and the calculated CIE coordinates variation is shown in **Figure 6**a to illustrate the color change versus angle. Same coordinates are plotted versus angle of incidence in Figure 6b.

The total crystallization energy is summarized in **Table 1** for each arm for both sequential and abrupt color change. The total energy to change the color of all four arms is obviously higher in sequential process. This table also shows different combination of excitation ports used to partially crystallize each arm of the "M" sign.

3. Methods and Design

To understand the optical response of the multilayer structure and how to enhance the light contrast when each layer of GeTe undergoes phase transition, transfer matrix method is

**ADVANCED
SCIENCE NEWS**
www.advancedsciencenews.com

**ADVANCED
OPTICAL
MATERIALS**
www.advopticalmat.de

Figure 5. Color transitions for the left arm of the "M" sign reflector when the device is excited from port (1) and (4). a) Right and middle arms were already transitioned to CC state and both GeTe layers are still amorphous in the left arm (AA). b,c) Two intermediate states were achieved by applying controlled voltage pulses between port (1) and (4) to transition the left arm to AC (b) and CA (c) states, respectively. Other three arms were kept at CC state with higher conductivity during these transitions. d) Finally, left arm is transitioned to CC states from (c), which shows the matched colors to all other three arms that were kept at CC state for all these transitions. The images were digitally zoomed due to optical zoom.

employed. For this purpose, matrix "M" associated with each layer is derived as[40]

$$M = \prod_n \begin{bmatrix} e^{\beta_n} & r_{n,n+1}e^{\beta_n} \\ r_{n,n+1}e^{-\beta_n} & e^{-\beta_n} \end{bmatrix} \quad (1)$$

$r_{n,n+1}$ is the light reflection from nth interface and β_n is the phase accumulation in the nth layer. These parameters are defined as

$$r_{n,n+1} = \left(\frac{k_n - k_{n+1}}{k_n + k_{n+1}} \right) \quad (2)$$

$$\beta_n = e^{ik_n t_n} \quad (3)$$

where k_n is the wavevector in layer n and t_n is the nth layer thickness. Wavevector (k_n) is $n_n \times \cos(\theta)$ for s-polarization and $n_n/\cos(\theta)$ for p-polarization. θ is light incidence angle. Total light reflection of the stack is then calculated as

$$R = \left| \frac{M_{01}}{M_{00}} \right|^2 \quad (4)$$

Such a reflection is dependent on the thickness and refractive index of the each layer integrated in the stack, which we briefly discuss here. First, reflection peak located at wavelength range from 600 nm–800 nm, which corresponds to optical cavity mode, could be tuned by changing the thickness of phase-shifter film (SiO$_2$) (**Figure 7**). The lossy GeTe film sitting on top of the SiO$_2$
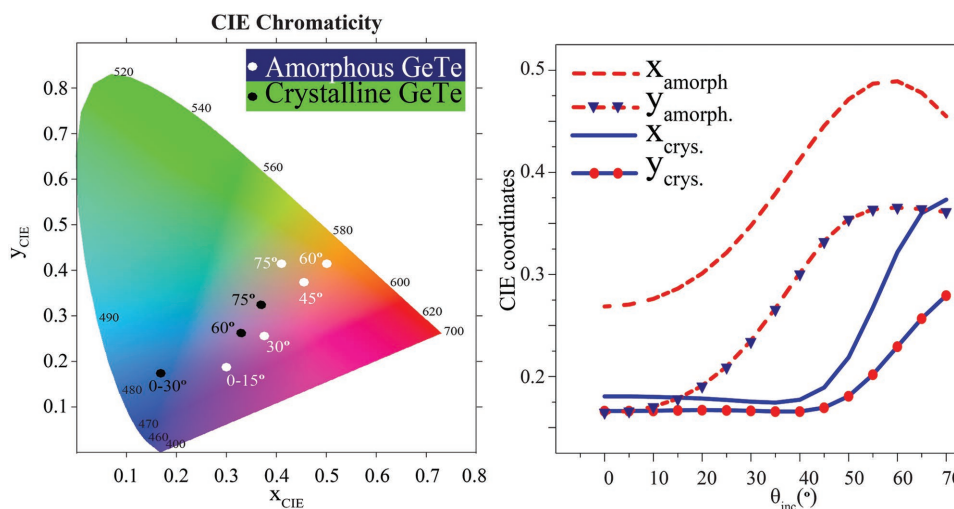
Figure 6. a) Experimental data showing angle sensitivity of the reflective colors for both phases of GeTe shown with white for amorphous and black for crystalline phase at room temperature using spectroscopic ellipsometry. b) CIE standard coordinates variation versus incident angles for designs consisting of amorphous and crystalline GeTe films.

Table 1. Phase transition energy consumption and heater resistance change for sequential and abrupt color switching of "M" sign.

Transitions		Excitation ports	R_0 [Ω]	$R_{post\text{-}cryst.}$ [Ω]	E [nJ]
Sequential	Right arm	1 and 2	80	50	25
	Right and middle arms	1 and 3	150	98	8.2
	All arms	1 and 4	180	125	11.2
Abrupt	All arms	1 and 4	220	124	11.6

layer and Pd film on the bottom make an asymmetric Fabry–Pérot cavity. This acts as a filter, which only permits constructive reflection of the optical wavelength twice that of the node spacing. Thus, it is clear that changing the thickness of SiO$_2$, in other word moving this node up and down with reference to the bottom palladium reflector, tunes the position of this peak. The multilayer device reflections in all four states are shown in Figure 7a–d. Due to high reflectivity of the top GeTe layer when it is crystalline, this tunability is very significant for the CC and CA states (see Figure 7a,b). However, this cavity response dependency on the SiO$_2$ layer is clearly shown for the case of AC and AA states when top GeTe layer is amorphous in Figure 7c,d. Figure 7c shows how the reflection peak tunes with different phase shift layer thickness (h_{PS}) and refractive index (n_{PS}) value

$$\lambda_{maximum} = 2 \times h_{PS} \times n_{PS} \tag{5}$$

For the case of SiO$_2$ with 250 nm thickness, this peak is located at ≈ 700 nm, causing the maximum color dynamic dependency on refractive indexes of GeTe layers. As shown in Figure 7d, the peak exists at the same wavelength for both

AC and AA states. The position of the peak is not tunable with GeTe phase transitions but the mode is more confined when the bottom layer is crystalline (AC state, Figure 7c).

Proper design, however, will produce several reflection dips (total light absorption) within the visible spectrum following thin film resonance. This resonance is the result of making the numerator zero in the closed form formula for a thin lossy film sitting on a metal substrate[30]

$$r = \frac{r_{12} + r_{23}e^{i\phi_1}}{1 + r_{12} \times r_{23}e^{i\phi_1}} \tag{6}$$

where ϕ_1 is light phase accumulated in the thin film which is equal to $2\pi n_2 h_2/\lambda$. r_{12} and r_{23} are reflection coefficient at top and bottom interfaces, respectively. Once cascaded, Equation (5) can be used for thin GeTe film separated from bottom reflector with a phase shifter as

$$\overline{r}_{123} = \frac{r_{12} + R_{34}e^{i\phi_1}}{1 + r_{12} \times R_{34}e^{i\phi_1}} \tag{7}$$
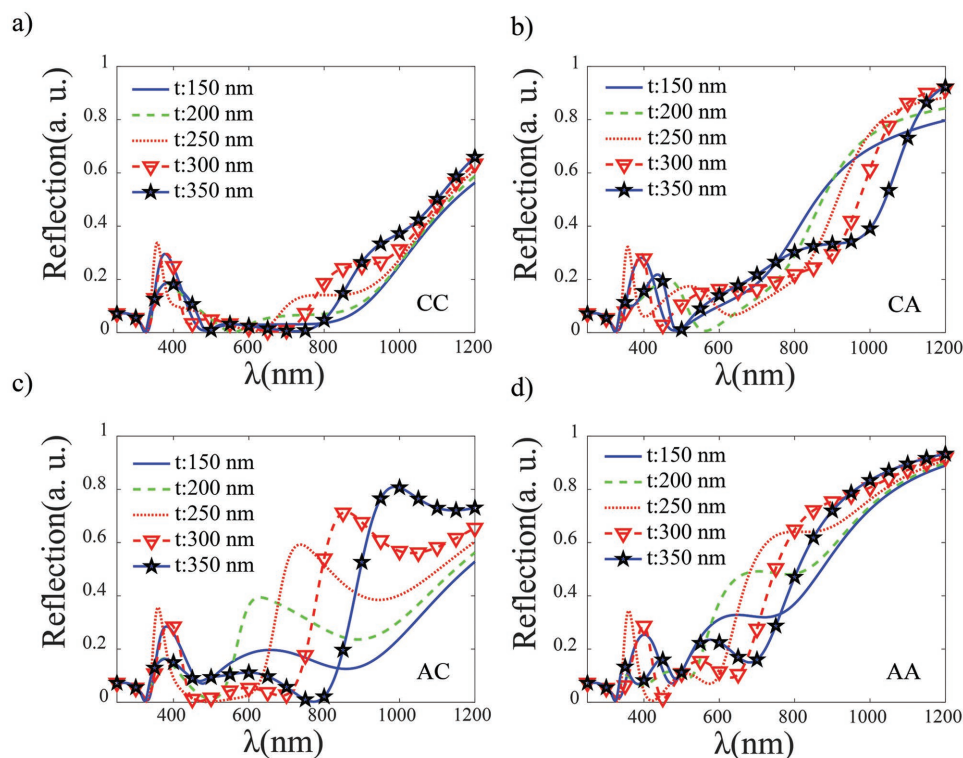
Figure 7. Device reflection in vis–NIR region with different SiO$_2$ thicknesses. (Incident angle: 50°).

where R_{34} is the reflection from the SiO_2/GeTe interface and can be calculated from the same general Equation (6). Adding more layers to this equation allows multiple thin film resonance within the visible wavelength depending on the thicknesses of different layers. The total device reflection in different states of the GeTe layers (CC, CA, AC, and AA) when the thickness of bottom TiO_2 layer (with nominal thickness of 60 nm) is varied between 40 and 100 nm, is shown in **Figure 8**. The change in the thickness of bottom TiO_2 layer that separates two GeTe layers has a higher impact on tuning the light reflection at the visible region. This figure shows that multilayer device supports three thin film resonances within the visible region. The wavelength of these near-perfect absorptions depends on the thicknesses and refractive indexes of each layer. Thus, tuning the refractive index of the GeTe layers results in multicolor by tuning the position of these reflection dips. The sensitivity of the wavelength at which these dips are located to the GeTe refractive index, depends on the TiO_2 spacer sandwiched between GeTe layers, SiO_2 phase shifter layer, as well as top antireflection coating. However, it is clear that the maximum color sensitivity to TiO_2 thickness is when both GeTe layers are amorphous and thus less lossy (see the oblique line in Figure 8d).

The other dip located at 380 is due to the top GeTe layer which is why it exists in all four states. The corresponding reflection dip and the peak at 400 nm are not significantly tunable with GeTe phase transition due to low contrast in the real part of refractive index (Figure 1a). However, by switching the state of these thin GeTe films from crystalline to amorphous, its refractive index is modulated and subsequently the amount of reflected red color could be enhanced.

This results in a reddish color reflected from the surface of the device.

4. Conclusion

In conclusion, a color reflector was demonstrated using multiple layers of a phase change material (GeTe) sandwiched between TiO_2 films. By thermally switching the phase of the GeTe layer, multiple colors were achieved within the same pixel with zero power needed to retain each color, making the scheme attractive for low refresh rate display systems. Four different colors ranging from blue to red were achieved using two ultrathin layers of GeTe with 8 and 20 nm thickness in a stack by selectively switching each layer between crystalline and amorphous states. We demonstrated for the first time that the phase transition temperature of GeTe can be tuned by changing its thickness value, a method used to achieve more than two colors in a stack consisting of multilayers of GeTe.

Supporting Information

Supporting Information is available from the Wiley Online Library or from the author.

Acknowledgements
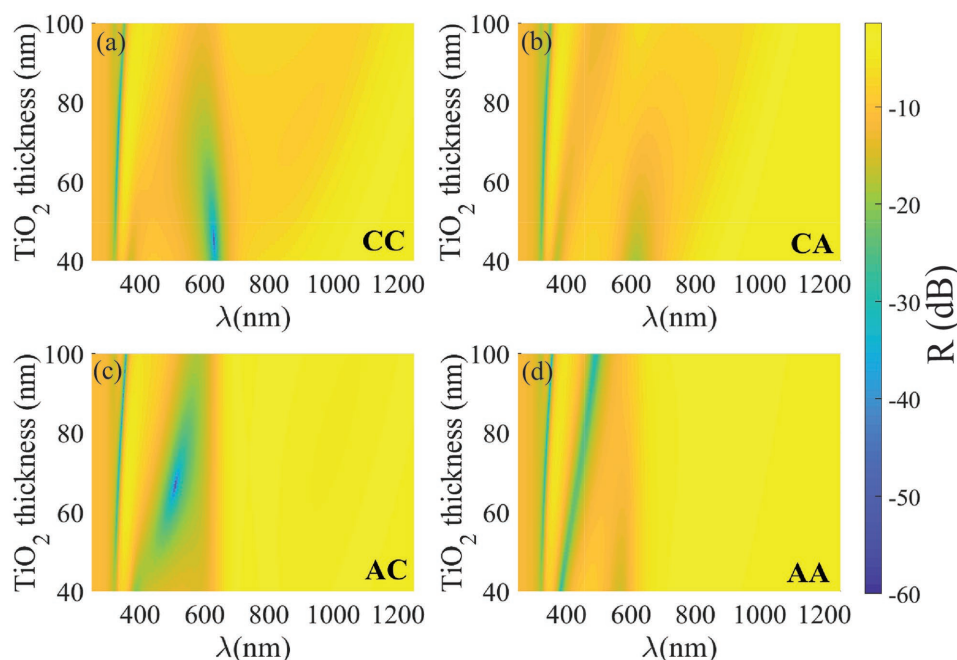
Figure 8. Multilayer device reflection in logarithmic scale to show the thin film resonances with varied bottom TiO_2 layer thickness. The dips in the reflection correspond to total light absorption which is mostly visible when both GeTe layers are amorphous (AA, (d)), with more than 40 dB absorption within the visible wavelengths at 50° incident angle.

Conflict of Interest

The authors declare no conflict of interest.

Keywords

[1] J. Li, T. Nakagawa, J. Macdonald, Q. Zhang, H. Nomura, H. Miyazaki, C. Adachi, *Adv. Mater.* **2013**, *25*, 3319.
[2] M. Zhu, C. Yang, *Chem. Soc. Rev.* **2013**, *42*, 4963.
[3] K.-T. Lee, S. Seo, J. Y. Lee, L. J. Guo, *Adv. Mater.* **2014**, *26*, 6324.
[4] Y. S. Do, J. H. Park, B. Y. Hwang, S.-M. Lee, B.-K. Ju, K. C. Choi, *Adv. Opt. Mater.* **2013**, *1*, 133.
[5] G. H. Gelinck, H. E. A. Huitema, E. van Veenendaal, E. Cantatore, L. Schrijnemakers, J. B. van der Putten, T. C. Geuns, M. Beenhakkers, J. B. Giesbers, B.-H. Huisman, E. J. Meijer, *Nat. Mater.* **2004**, *3*,106.
[6] T. Sekitani, H. Nakajima, H. Maeda, T. Fukushima, T. Aida, K. Hata, T. Someya, *Nat. Mater.* **2009**, *8*, 494.
[7] H. Cho, S.-H. Jeong, M.-H. Park, Y.-H. Kim, C. Wolf, C.-L. Lee, J. H. Heo, A. Sadhanala, N. Myoung, S. Yoo, S. H. Im, *Science* **2015**, *350*, 1222.
[8] E. K. Chan, T. Chang, T.-C. Fung, J. Hong, C. Kim, J. Ma, Y. Pan, S.-G. Wang, B. Wen, *J. Microelectromech. Syst.* **2017**, *26*, 143.
[9] L. Chang, F. Chen, X. Zhang, T. Kuang, M. Li, J. Hu, J. Shi, L. J. Lee, H. Cheng, Y. Li, *ACS Appl. Mater. Interfaces* **2017**, *9*, 16553.
[10] J. Lee, H.-F. Chen, T. Batagoda, C. Coburn, P. I. Djurovich, M. E. Thompson, S. R. Forrest, *Nat. Mater.* **2016**, *15*, 92.
[11] Z. Shen, P. E. Burrows, V. Bulović, S. R. Forrest, M. E. Thompson, *Science* **1997**, *276*, 2009.
[12] J. Hong, E. Chan, T. Chang, T.-C. Fung, B. Hong, C. Kim, J. Ma, Y. Pan, R. Van Lier, S. G. Wang, B. Wen, *Optica* **2015**, *2*, 589.
[13] J. Ma, *Displays* **2015**, *37*, 2.
[14] K.-T. Lee, J.-Y. Jang, S. J. Park, U. K. Thakur, C. Ji, L. J. Guo, H. J. Park, *Optica* **2016**, *3*, 1489.
[15] R. J. Mortimer, *Chem. Soc. Rev.* **1997**, *26*, 147.
[16] F. M. Raymo, M. Tomasulo, *Chem. - Eur. J.* **2006**, *12*, 3186.
[17] C.-G. Granqvist, *Nat. Mater.* **2006**, *5*, 89.
[18] A. Zakery, S. Elliott, *J. Non-Cryst. Solids* **2003**, *330*, 1.
[19] Y. Li, Y. Zhong, L. Xu, J. Zhang, X. Xu, H. Sun, X. Miao, *Sci. Rep.* **2013**, *3*, 1619.
[20] D. D. Ordinario, E. M. Leung, L. Phan, R. Kautz, W. K. Lee, M. Naeim, J. P. Kerr, M. J. Aquino, P. E. Sheehan, A. A. Gorodetsky, *Adv. Opt. Mater.* **2017**, *5*, 1600751.
[21] M. Humar, M. Ravnik, S. Pajk, I. Muševič, *Nat. Photonics* **2009**, *3*, 595.
[22] D.-K. Yang, *Fundamentals of Liquid Crystal Devices*, Wiley, Hoboken, NJ, USA **2014**.
[23] K. Ramesh, S. Asokan, K. Sangunni, E. Gopal, *Appl. Phys. A: Mater. Sci. Process.* **1999**, *69*, 421.
[24] M. Jafari, M. Rais-Zadeh, *Opt. Lett.* **2016**, *41*, 1177.
[25] M. Liu, H. Y. Hwang, H. Tao, A. C. Strikwerda, K. Fan, G. R. Keiser, A. J. Sternbach, K. G. West, S. Kittiwatanakul, J. Lu, S. A. Wolf, *Nature* **2012**, *487*, 345.
[26] K. Shportko, S. Kremers, M. Woda, D. Lencer, J. Robertson, M. Wuttig, *Nat. Mater.* **2008**, *7*, 653.
[27] P. Hosseini, C. D. Wright, H. Bhaskaran, *Nature* **2014**, *511*, 206.
[28] S. Yoo, T. Gwon, T. Eom, S. Kim, C. S. Hwang, *ACS Photonics* **2016**, *3*, 1265.
[29] N. Raeis-Hosseini, J. Rho, *Materials* **2017**, *10*, 1046.
[30] M. A. Kats, R. Blanchard, P. Genevet, F. Capasso, *Nat. Mater.* **2013**, *12*, 20.
[31] Y. Meng, J. K. Behera, Y. Ke, L. Chew, Y. Wang, Y. Long, R. E. Simpson, *Appl. Phys. Lett.* **2018**, *113*, 071901.
[32] M. Wuttig, M. H. Bhaskaran, T. Taubner, *Nat. Photonics* **2017**, *11*, 465.
[33] D. Yu, J. Wu, Q. Gu, H. Park, *J. Am. Chem. Soc.* **2006**, *128*, 8148.
[34] N. Yamada, T. Matsunaga, *J. Appl. Phys.* **2000**, *88*, 7020.
[35] A. Tittl, A.-K. U. Michel, M. Schäferling, X. Yin, B. Gholipour, L. Cui, M. Wuttig, T. Taubner, F. Neubrech, H. Giessen, *Adv. Mater.* **2015**, *27*, 4597.
[36] K. N. Chen, L. Krusin-Elbaum, D. M. Newns, B. G. Elmegreen, R. Cheeck, N. Rana, A. M. Young, S. J. Koester, C. Lam, *IEEE Electron Device Lett.* **2008**, *29*, 131.
[37] K. V. Sreekanth, S. Han, R. Singh, *Adv. Mater.* **2018**, *30*, 1706696.
[38] M. Wang, Y. Shim, M. Rais-Zadeh, *IEEE Electron Device Lett.* **2014**, *35*, 491.
[39] X. Zhou, J. Kalikka, X. Ji, L. Wu, Z. Song, R. E. Simpson, *Adv. Mater.* **2016**, *28*, 3007.
[40] M. Born, E. Wolf, *Principles of Optics*, 4th ed., Pergamon Press, Oxford **1970**.